Comparison of LoRaWAN Classes and their Power Consumption

Phui San Cheong [*], Johan Bergs[*], Chris Hawinkel[§], Jeroen Famaey[*]
[*] IDLab, University of Antwerp – imec, Antwerp, Belgium
[§] Nokia Bell Labs, Antwerp, Belgium
Email: jeroen.famaey@uantwerpen.be

***Abstract*—Many Internet of Things (IoT) applications benefit greatly from low-power long-range connectivity. A promising technology to achieve the low-power and long-range requirements is seen in LoRaWAN, a media access control (MAC) protocol maintained by the LoRa Alliance and leveraging Semtech's patented LoRa radio modulation technology. LoRaWAN provides three different device classes (A, B and C), which provide a trade-off between performance (i.e., throughput and latency) and energy consumption. This paper offers a theoretical and experimental comparison of these classes. The objective of the quantitative experiment was twofold: to verify the published current levels of different operating modes in a LoRa chip's datasheet and to compare the battery lifetime for the LoRa class A and C modes of operation. We used a high-end current sensing circuit to gather the voltage levels and temporal variation with increasing payload sizes and spreading factors. Using the Ohmic Law, the energy drain can be calculated and compared across the different spreading factors (SF) and classes.**

Keywords—Internet of Things (IoT); LoRa; LoRaWAN; LPWAN

I. Introduction

LoRaWAN [1] was developed to overcome the challenges of IoT applications. One of the key differentiators of the LoRAWAN protocol is its long-range connectivity despite being low-power. LoRaWAN claims connectivity up to 15 km Line-of-Sight (LOS), much further than Wi-Fi, ZigBee, and Bluetooth, which feature ranges of up to 100 meters. However, the actual useful range might be a bit shorter (± 10 km) [2].

There are other Low-Power Wide-Area Network (LPWAN) protocols, such as Sigfox, Ingenu and DASH7, which manage to achieve a similar range. However, LoRa(WAN) offers a great deal of flexibility due to its support for multiple spreading factors (SFs) and device classes. As such, this paper focuses on LoRa(WAN), and investigates the trade-offs offered by this flexibility.

Even though this paper only focuses on LoRaWAN, it is important to realize that LoRaWAN is not a network technology that is able to fulfil all the different requirements for a IoT deployments [3].

Depending on the concrete situation, the requirements can be very different, implicating that one of the other networks (e.g. Sigfox) might be better suited for that particular use case. In [4], a comparison is made on throughput and range for two different technologies: chirp spread spectrum (CSS), as used by LoRa and ultra-narrowband (UNB) as used by Sigfox. This study shows that an UNB network performs better for long range communication, at the expense of available throughput for each device. CSS networks, on the other hand, are better suited for higher bitrate applications that do not require such a long range.

An important aspect of IoT networks is scalability. As it is expected that there will be many more IoT devices in the coming years, an IoT network should be able to cope with a large number of devices connecting to it. In [5], [6] and [7], the scalability of LoRa networks is studied, and all these conclude that LoRa does not scale extremely well. Solutions for this problem are described, however they require further study.

The long range with low power usage offered by the LoRaWAN specification is achieved via 2 techniques: (i) the LoRa Modulation technology and (ii) an Adaptive Data Rate (ADR) selection, which are both discussed in Section II. The LoRaWAN protocol and the overall network architecture are also described in the same section. The experiment conducted to verify and validate the power consumption of device classes A and C using a known LoRa device are explained in Section III. The results of this experiment and some conclusions are discussed in Section IV and Section V, respectively.

II. LoRaWAN Overview

A. LoRaWAN Protocol and Architecture

At the core of every LoRaWAN network is the network server. It can be connected to many LoRaWAN gateways, which act as "base stations" or "access points" for the end-devices at the front-end and one or more application servers at the back-end, processing the data generated by the end devices, giving rise to a star-to-star topology, as can be seen in Figure 1 [8]. A more detailed description of the LoRaWAN network architecture can be found in [9].

B. LoRa Modulation technique (by Semtech Corporation)

The LoRa Modulation technique is patented by Semtech Corporation, a supplier of analogue and mixed-signal semiconductors and integrated circuits. The modulation makes use of a chirp signal, which has a frequency that increases or decreases over time. The chirp signal normally has a higher frequency level than the data signal. The data signal is encoded on the chirp signal and the resulting modulated signal is spread over a wide band beyond the original data signal's bandwidth.

978-1-5386-2256-8/17/$31.00 ©2017 IEEE

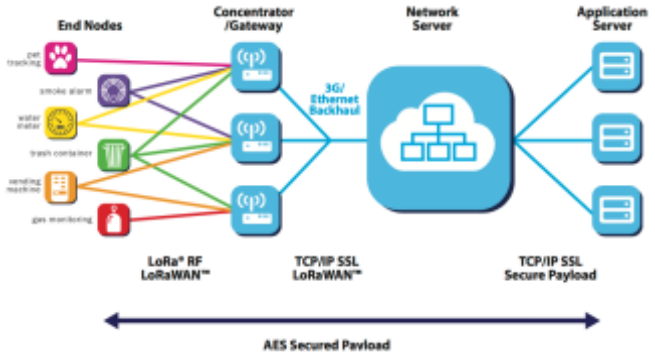

Figure 1 – LoRaWAN Architecture

In [11], Semtech describes that "In information theory, the Shannon-Hartley theorem states the maximum rate at which information can be transmitted over a communications channel of a specified bandwidth in the presence of noise." Furthermore, as in spread spectrum applications, the signal-to-noise ratio is small (S/N << 1), it is demonstrated that, using the LoRa modulation technique, "it can be seen that to transmit error free information in a channel of fixed noise-to-signal ratio, only the transmitted signal bandwidth need be increased."

The relationship between bitrate, symbol rate, bandwidth and spreading factor for LoRa modulation can be expressed as follows:

$$R_s = \frac{BW}{2^{SF}}, \text{ and } R_b = SF * \frac{\frac{4}{4+CR}}{\frac{2^{SF}}{BW}} \text{ bits/s} \quad (1)$$

where:

R_s = symbol rate (symbols/sec)
BW = modulation bandwidth (Hz)
SF = spreading factor (7…12)
R_b = data bit rate (bits/sec)
$\frac{4}{4+CR}$ = Rate Code

The modulation scheme employs orthogonal spreading factors, which enable multiple spread signals to be transmitted at the same time and on the same channel with minimal degradation on the receiver sensitivity. This allows LoRaWAN networks to achieve a link budget up to 157 dB and a sensitivity up to -137 dBm 0.

C. Adaptive Data Rate

A second technique used in a LoRaWAN network is the Adaptive Data Rate. Essentially a power-saving mechanism, the data rate and Radio Frequency (RF) output power are adjusted in accordance to the distance of the node from the gateway. The nodes close to the gateway use a higher data rate (with shorter Time-on-Air) and a lower RF output power. The ADR method is able to accommodate changes in the network infrastructure and support varying path loss. As can be seen in [1], supported data rates range from 0.3 kbps to 50 kbps. The ADR mechanism tries to use the highest possible data rate at all times. Sending at a higher data rate (i.e., using a lower SF) reduces the Time-on-Air of a packet, thus reducing the energy needed to transmit that packet. However, increasing the data rate also increases the chance that a transmission is not received correctly due to interference.

D. Device classes

Three classes of LoRa devices exist, named A, B and C. Class A and Class B are normally battery-powered, whereas Class C is mains-powered. By default, a LoRa device is a Class A device with power saving capabilities, unless it is specifically configured to operate in class B or C mode. The major difference in the three modes of operation is in the reception of packets (i.e. sent from the gateway to the device). Class A devices only have two very short receive windows after they have transmitted a packet. After the receive windows, the class A device goes to sleep in order to conserve energy. In addition to class A device receive windows, class B devices open extra receive windows at scheduled intervals. The receive windows are synchronized by beacons sent from the gateway. Last, class C devices, as they are usually not battery-powered, can afford to continuously have their radio in receive mode (as long as they are not transmitting themselves), allowing for instantaneous transmission of data towards a device without having to wait for a receive window to open. Figures 2, 3 and 4 highlight the operation of the receive windows for class A, B and C devices respectively. The different operating modes influence the energy drain and consequently the battery lifetime of such a device. Class B devices are not included in the evaluation of this paper due to unavailability of a class B driver implementation at the time of the experiment.

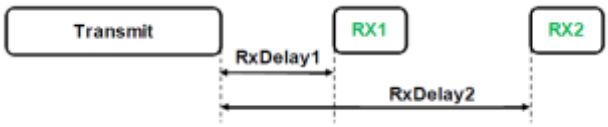

Figure 2 - Class A device receive windows

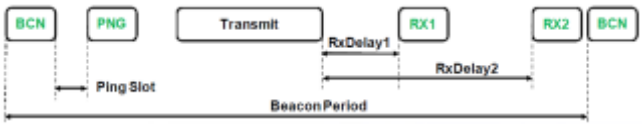

Figure 3 - Class B device receive windows

Figure 4 - Class C device receive windows

III. Experiment Setup

A. Description

To compare the power consumption of class A and C devices,

we set up an experiment with the aim to verify the published current levels in the iM880B-L datasheet [10] for the four different operating modes of that chip (Transmit, Receive, Idle and Sleep). In addition, calculations are made to compare the energy drain between the classes when operating in Class A and C, and to predict the battery lifetime of the devices between Spreading Factors 7 and 11 when operating in Class A.

The demo board we used for the experiment comes with an additional adapter PCB, called iM880A, which is soldered on. It contains a transceiver (SX1272) and a Microcontroller Unit (MCU) with an STM32L151CB ARM Cortex M3 processor. This PCB is connected with an antenna through the RF interface. The Demoboard itself contains buttons, LEDs, sensors, a pin for connecting a GPS receiver and an external header comprising of all iMST iM880A module pins. Within the Microcontroller Unit (MCU), additional communication interfaces are supported such as Inter-Integrated Circuit (I2C) bus, Universal Asynchronous Receiver Transmitter (UART) and Serial Peripheral Interface (SPI).

A high-end resistive current sensing circuit is used to measure the voltage drop across a resistor. The Device Under Test (DUT) is the iM880B-L board with Antenna, yielding a fully functional LoRa Alliance certified module. The voltage drop measured is proportional to the system load current as per Ohm's Law (i.e., V = I x R). As low current levels are expected especially in sleep mode, a low-ohmic high-precision 10 Ω sense resistor is connected in series with the DUT. The resistance must be sufficiently high to induce a voltage drop within the resolution of the available measuring instrument but not too high as to affect the DUT's performance. An oscilloscope is then connected to measure the iM880B-L's voltage level.

In order to be able to send and receive LoRaWAN messages on our DUT, a Multitech LoRa indoor gateway was setup in another room, at a distance of about 10m from the test setup.

B. Voltage Measurements

The energy drain is expressed in mAh. This is easily calculated from the voltage levels and the duration for each operating mode in the voltage graphs. We compared LoRa Class A and C with varying payload sizes and spreading factors. From there, we calculate the values for mAh across 10 years (given that the reference from LoRa proponents and vendors is typically a 10-year lifetime for battery-operated LoRa sensors).

In Figure 5, the voltage graph for Over-the-Air Activation (OTAA) is shown. There are two reception windows opened in OTAA, which is not always the case if a message is received in RX1 and the message passes the Message Integrity Code (MIC) verification. In OTAA, the uplink message transmitted is called JOIN Transmit and the downlink message received can be JOIN Accept 1 or 2 (dependent on the delay set by network server). The downlink message in this case is received in RX2. There is a slight bump of high signal just before the Transmit signal, which indicates that the sensors on the board are activated.

In Figure 6, the voltage graph for Class A is as shown. When the device is configured as Class A, a voltage pattern with 1 Transmit (TX) high signal and 2 trailing Receive (RX) high signals, is observed. The time interval for RX1 Delay is 1 second and for RX2 Delay is 2 seconds, as recommended by the LoRaWAN specification. The voltage level for idle mode is higher than for sleep mode because essentially Idle Mode is just Sleep Mode with RC oscillator on the MCU. From [4] and [7], it should be noted that in the EU863 - EU870 band, the RX2 is always operating with the following parameters: 869.525 MHz /DR0:250bps, SF12, 125 kHz bandwidth.

In Figure 7, the voltage graph for a Class C device is shown. When the device is configured as Class C, a voltage pattern with 1 TX high signal and a plateau can be seen before a drop-in voltage level to a new RX2 continuous level. The plateau consists of RX2 and RX1 as discussed earlier in Class A. These two slots typically have the same reception parameters, with the same channel and data rates. The RX2 in the plateau is observed to be different than the RX2 continuous. The default RX2 continuous reception parameters are 869.525 MHz, SF 9, 125 kHz bandwidth and up to 27 dBm (Equivalent Isotropically Radiated Power – EIRP), the same used for beacon transmission in Class B.

The Time-on-Air of a packet obviously increases with the payload size. Additionally, for a fixed payload size, the Time-on-Air also increases as the Spreading Factor (SF) increases. At lower data rates, the Time-on-Air needs to be increased to transmit the same payload completely. From [12], this relationship can be formulated as follows:

Figure 5 - Over-the-Air Activation

Figure 7 - Voltage graph for a class A device

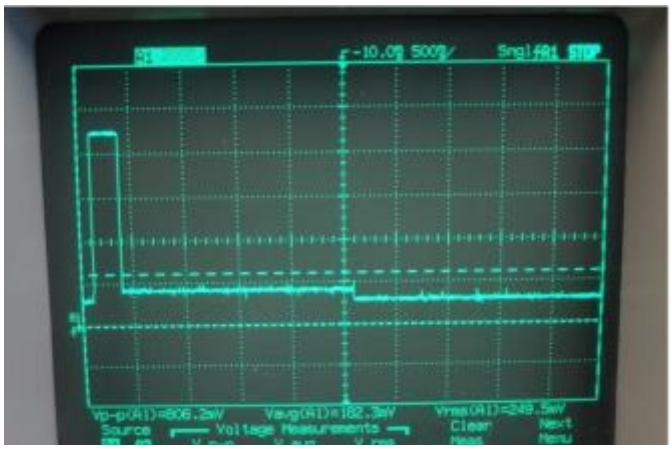

Figure 6 - Voltage graph for a class C device

$$ToA = T_{preamble} + T_{sym} * (8 + max(ceil\left(\frac{8 * (PL) - 4 * SF + 28 + 16 - 20 * H}{4 * (SF - 2 * DE)}\right) * (CR + 4),0)$$

where

- PL is the number of payload bytes
- SF is the spreading factor
- H=0 (header enabled) and H=1 (header disabled)
- DE=1 when low data rate optimisation is enabled, DE=0 when it is disabled
- CR is coding rate used from 1 to 4

C. Current Measurements

The benchmark current levels for Class A & C are obtained from [10]. The current level for TX mode is 117 mA (minimum level is assumed) and for sleep mode it is at 1.8 μA.

In the experiment, we observed that the current levels for the different operating modes do not show any apparent trend and appear to display the same order of magnitude across payload sizes and SF. Therefore, an average is taken for all the readings in their respective LoRa classes. We verified the relative current levels for the different consumption modes. The measured voltage/current levels are comparable for TX, Idle and RX modes. In our experiment, the current measured for Class A sleep mode was 1.27 mA, 3 orders of magnitude higher than the benchmark value (1.8μA). This difference can probably be attributed to the device not really being in deep sleep mode, although further investigation is needed to confirm this. In [6] it is explained that LoRa has different categories for low power mode, namely "Deep Sleep" and 'Standby". In Deep Sleep mode, the supply current is 1 μA with an additional 0.8 μA consumption from the MCU, which has to operate the Real-time Clock (RTC). In Standby Mode, the supply current mentioned is 1.6 mA, which is a value that is much closer to the observed readings. We speculate that although the automated power savings were on, the low power mode for the device was set to standby instead of sleep mode.

Because of the very large difference between the theoretical (benchmark) values and the actual measured values for sleep mode, we will use the theoretical values for the battery lifetime prediction below, as we believe the measured values are probably caused by a misconfiguration in the driver and would yield results that are very different from those obtained with the benchmark figures. For all other operating modes, however, the measured values are used. The values mentioned in this paper are obtained by transmission of unconfirmed data. Additional traffic caused by MAC Commands/Responses and Retransmissions is not considered. In the experiment, only SF7, 9 and 11 are used.

D. Battery Lifetime Prediction

The battery lifetime prediction assumptions are based on the utilization of an LR03 battery with a capacity of 2000 mAh. In our experiment, we used various payload sizes for the packets transmitted, between 25 and 115 bytes.

Figures 8 – 11 show the total power requirement for a class A and Class C device, respectively, for a 10-year period. In Figure 8, we assume a class A device that uses SF7 for transmission. The different lines show the different power requirements for increasing payload sizes. The X-axis depicts increasing intervals between each subsequent packet transmission. In Figure 9, the same class A device is considered, but this time using SF11. Figures 10 and 11 show the same graphs, but this time for a class C device. The figures show that for Class A, using a higher SF implies a significantly higher energy consumption (lower battery lifetime), while in Class C, the power consumption is almost the same.

In the experiment, we observed that the duration for Idle and RX modes are fairly consistent. We observed the voltage pattern for a class A device, spending most of its time in sleep mode and for a class C device, spending most of its time in RX2 mode. The difference between the benchmark values and the experiment values for Class C is small compared to the difference observed for Class A. Therefore, in the power requirement figures, the measured values are included for the class C device, but for class A device graphs, measured values for all operating modes except sleep mode are used. The actual TX mode current level we measured for both classes was lower than the benchmark value(95 vs. 117mA), but this has little influence on overall energy consumption.

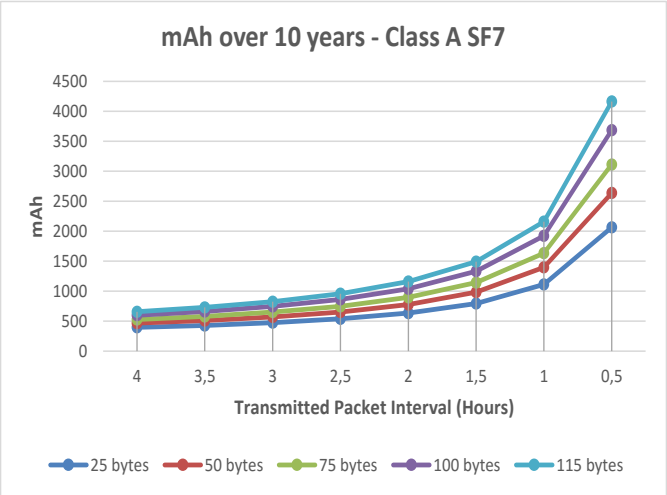

Figure 8 - Experiment values of required mAh over 10 years for varying transmitted packet intervals (Class A - SF7)

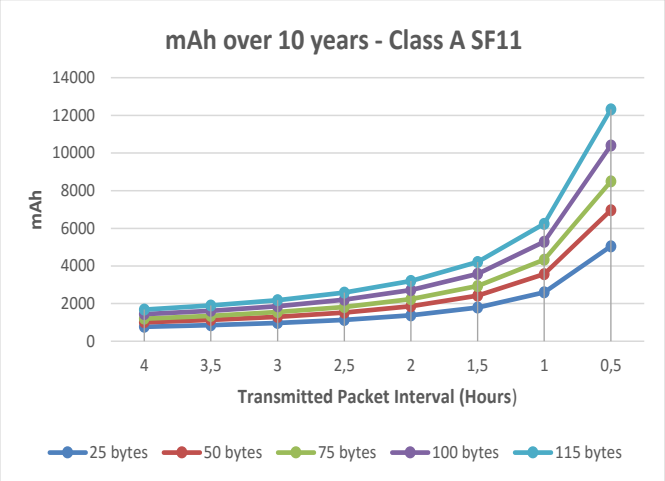

Figure 9 - Experiment Values of required mAh over a period of 10 years for varying transmitted packet intervals (Class A-SF11)

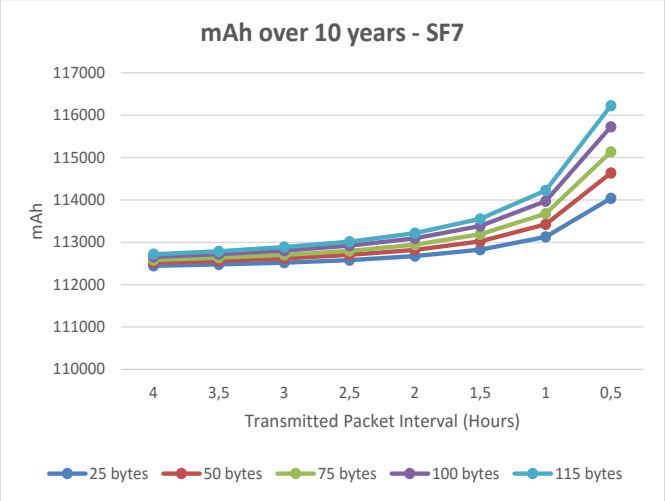

Figure 10 - Experiment Values of required mAh over a period of 10 years for varying transmitted packet intervals (Class C-SF7)

As can be seen from the graphs, for a class A device, the interval between each subsequent packet transmission has a large impact on the total power consumption. Using a higher SF significantly increases the total power consumption. If we assume to use an LR03 battery with a 2000 mAh capacity, in order to ensure a 10-year operational life of the device, care must be taken to use a suitable spreading factor, limit the amount of packet transmissions and also, keep the payload size as small as possible (i.e. encode the information that needs to be transmitted in as few bytes as possible). The last two requirements (payload size and packet transmission interval) can be fully controlled by the device manufacturer as they are purely application-dependent. The spreading factor, however, may depend on the network conditions. If the device is used in a location with relatively bad LoRaWAN coverage, using a lower SF might not be possible. From the graphs, it is also clear that using a battery-powered class C device is not feasible for long-term deployment. This is not a concern, however, as class C devices are normally designed to be connected to a mains power supply.

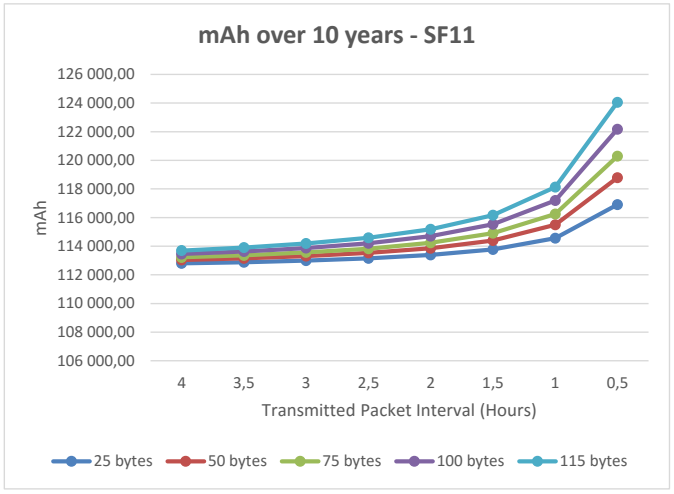

Figure 11 - Experiment Values of required mAh over a period of 10 years for varying transmitted packet intervals (Class C-SF11)

Figure 12 - HCI Log File showing ADR and Channel Hopping Sequence

IV. Observations

During the experiment, we also observed the LoRaWAN ADR, duty cycle control and channel hopping sequence behaviour.

Figure 12 shows the Host Controller Interface (HCI) log file when several packets are transmitted and the network connectivity is considered as stable. For each packet to transmit, the end device changes channel in a pseudo-random fashion.

The 3 mandatory frequency channels that are used with the DUT are 868.1 MHz, 868.3 MHz and 868.5 MHz. The resulting frequency diversity makes the system more robust to interference. The link quality is characterised by Received Signal Strength Indicator (RSSI). When measured in decibels, or dBm on a logarithmic scale, the signal is better when it is closer to 0dBm. ADR kicks in by the MAC Command, *Link CheckAns* (line 24), to answer to a *LinkCheckReq* (a MAC Command transmitted by end-device) for link quality validation. *LinkCheckAns* contains the received signal power estimation indicating the quality of reception to the end device. When the link quality is good, it is possible to send data at a lower transmission power and higher data rate. The *LinkADRReq* transmitted by Gateway requests end device to change data rate, transmit power, repetition rate or channel. This can be seen in line 27. Subsequent packet transmission after line 27 occurs at SF 7 (with Data Rate of 11 kbps) instead of SF 9 (with Data Rate of 1.76 kbps).

Duty cycle control can be observed on the Status Box when we attempt to transmit immediately after a transmission. An error message would appear to indicate that the transmission was not successful due to duty cycle control and the sub-band is blocked. We would need to wait for the duration of the block before we can successfully transmit again. The duration of the block, $Toff_{subband}$ is defined as follows:

$$Toff_{subband} = \frac{TimeOnAir}{DutyCycle_{subband}} - TimeOnAir$$

V. Conclusion

In this paper, we investigated the power requirements of a LoRaWAN class A and class C device. Especially for class A devices, this is an important measure as such a device is typically battery powered and should be able to last up to 10 years on a single battery. In order to accurately measure the power consumption, we used a well-known LoRa board that can operate both in class A and class C mode. A high-end resistive current sensing circuit was used to measure the power consumption of the chip in different operating modes (TX, RX, idle and sleep). The measurements were subsequently compared to the benchmark figures of the chip. Here, we noticed that most figures matched rather well for TX, RX and idle modes. The figures for sleep mode, however, were much higher than the benchmark. We believe this is due to a misconfiguration of the chip during the experiments. Therefore, instead of using the measured values for sleep mode, we have used the benchmark figures for subsequent calculations. From the measured and benchmark figures, we have calculated the power requirements of the LoRa device both in class A and class C mode, using different modulation techniques and payload sizes, over a 10 year period.

The results from our measurements and power requirement calculations show that, for a class A device, it is possible to obtain the 10-year operational goal if care is taken to use the proper payload size, transmission interval and to use a spreading factor that is as low as possible.

Throughout the experiment, a fixed power output is used at 14 dBm. A further investigation on the behaviour of a LoRa Device with varying power output could be within the scope of future work. Also, clarifying the discrepancy between the measured and the benchmark sleep current levels needs further investigation.

[1] LoRa Alliance Wide Area Networks for IoT. *LoRa Alliance Website* [Online]. Available: https://www.lora-alliance.org/

[2] J. Petajajarvi, K. Mikhaylov, A. Roivainen, T. Hanninen and M. Pettissalo, "On the coverage of LPWANs: range evaluation and channel attenuation model for LoRa technology," *2015 14th International Conference on ITS Telecommunications (ITST)*, Copenhagen, 2015, pp. 55-59.
doi: 10.1109/ITST.2015.7377400

[3] F. Adelantado, X. Vilajosana, P. Tuset-Peiro, B. Martinez, J. Melia-Segui and T. Watteyne, "Understanding the Limits of LoRaWAN," in *IEEE Communications Magazine*, vol. 55, no. 9, pp. 34-40, 2017. doi: 10.1109/MCOM.2017.1600613

[4] B. Reynders, W. Meert, and S. Pollin, "Range and coexistence analysis of long range unlicensed communication," in *2016 23rd International Conference on Telecommunications (ICT)*, 2016, pp. 1–6.

[5] M. C. Bor, U. Roedig, T. Voigt, and J. M. Alonso, "Do LoRa Low-Power Wide-Area Networks Scale?," in *Proceedings of the 19th ACM International Conference on Modeling, Analysis and Simulation of Wireless and Mobile Systems - MSWiM '16*, 2016, pp. 59–67.

[6] D. Bankov, E. Khorov and A. Lyakhov, "On the Limits of LoRaWAN Channel Access," *2016 International Conference on Engineering and Telecommunication (EnT)*, Moscow, 2016, pp. 10-14. doi: 10.1109/EnT.2016.011

[7] O. Georgiou and U. Raza, "Low Power Wide Area Network Analysis: Can LoRa Scale?," in *IEEE Wireless Communications Letters*, vol. 6, no. 2, pp. 162-165, April 2017.

[8] Lora Alliance: A technical overview of LoRa and LoRaWAN [Online] https://docs.wixstatic.com/ugd/eccc1a_ed71ea1cd969417493c74e4a13c55685.pdf

[9] A. Augustin, J. Yi, T. Clausen, and W. M. Townsley, "A Study of LoRa: Long Range & Low Power Networks for the Internet of Things.," *Sensors (Basel).*, vol. 16, no. 9, Sep. 2016.

[10] WiMOD iM880B Datasheet. DocID: 4100/40140/0100 [Online]. http://www.wireless-solutions.de/images/stories/downloads/Radio%20Modules/iM880B/General_Information/iM880B_Datasheet_V1_0.pdf

[11] AN1200.22 – LoRa Modulation Basics. [Online]. Available: http://www.semtech.com/images/datasheet/an1200.22.pdf

[12] SX1272/3/6/7/8: LoRa Modem. *Designer's Guide AN1200.13*. [Online]. https://www.semtech.com/images/datasheet/LoraDesignGuide_STD.pdf

[13] SX1272/73: Wireless, Sensing & Timing. *Datasheet*.[Online].http://www.semtech.com/images/datasheet/sx1272.pdf

[14] *LoRaWAN Specification,* LoRa Alliance Standard v 1.0.2, 2016 July.

[15] LORIOT Website[Online].Available:https://www.loriot.io